Journal of Catalysis 260 (2008) 81–85

Contents lists available at ScienceDirect

Journal of Catalysis

www.elsevier.com/locate/jcat

Stepwise fabrication and architecture of heterogeneous 9-thiourea epiquinine catalyst with excellent enantioselectivity in the asymmetric Friedel–Crafts reaction of indoles with imines

Peng Yu, Jing He *, Lan Yang, Min Pu, Xiaodan Guo

State Key Laboratory of Chemical Resource Engineering, Beijing University of Chemical Technology, Beijing 100029, PR China

ARTICLE INFO

Article history:
Received 12 July 2008
Revised 27 August 2008
Accepted 5 September 2008
Available online 8 October 2008

Keywords:
heterogeneous catalysis
Asymmetric C–C formation
9-Thiourea epiquinine
Enantioselectivity
Friedel–Crafts reaction
Mesoporous silica

ABSTRACT

Heterogeneous 9-thiourea epiquinine catalysts are prepared by covalently anchoring 9-(3,5-bis(trifluoromethyl)phenylthiourea)epiquinine on mesoporous silica surfaces via mercapto linker. It is found that 9-thiourea epiquinine moieties are located comparably on the interior and exterior surfaces of SBA-15 while preferentially on the exterior surface of MCM-41. The heterogeneous 9-thiourea epiquinine are applied as catalysts in the asymmetric Friedel–Crafts reaction of indoles with imines. SBA-15 supported 9-thiourea epiquinine, with more catalytic sites inside the channels, is found more chemselective and enantioselective than the counterpart supported on MCM-41. The effects of solvents and molecule dimensions of both substrates on the reaction effectiveness and selectivity are also discussed.

1. Introduction

Cinchona alkaloids have become a matter of current interest [1,2] because of their applications as homogeneous organocatalysts in a variety of asymmetric nucleophilic processes, including conjugate addition [3–8], Michael addition [9,10], Mannich [11,12], Friedel–Crafts [13,14], aza-Henry [15], aza-Michael [16], and Diels–Alder [17] reactions. The separation and subsequent recycle of homogeneous catalysts are problematic, however, making the entire process economically nonviable for industrial applications. The immobilization of homogeneous catalysts to solid supports has thus become an important strategy to obtain heterogeneous catalysts retaining the active sites of homogeneous analogues while easily separated and recycled [18]. Some papers [19,20] have reported the heterogenization of chiral organic molecules using organic polymers and inorganic solids as supports. Mesoporous silica materials with well-defined uniform mesopores and readily modified surfaces have been attracting much attention as supports for chiral catalytic sites [21–26]. Enhanced enantioselectivities in the epoxidation reaction were observed on MCM-41 supported Mn(III) salen [21] and Cr(III) Schiff base complexes [22]. The Pd^{II} and Rh^{I} complexes immobilized in mesoporous silica were also found to exhibit superior performance in the enantioselective allylic amination of cinnamyl acetate [23,24]. The *ee* of the allylic amination of cinnamylacetate, for example, was enhanced from 64 to 91% by rhodium(I) complex supported in the nano-sized channels of MCM-41. Mesoporous materials have apparently been demonstrated promising for designing and exploiting industrially robust heterogeneous catalysts.

9-(3,5-bis(trifluoromethyl)phenylthiourea)epiquinine (abbreviated 9-thiourea epiquinine), a cinchona alkaloid-derived chiral bifunctional thiourea organocatalyst, is energetic in a large number of asymmetric C–C formation reactions. But its heterogenization has seldom been reported. This work, therefore, reports the immobilization of 9-(3,5-bis(trifluoromethyl)phenylthiourea)epiquinine on mesoporous SBA-15 and MCM-41 materials through a covalent bottom-up approach. The stepwise fabrication and the architecture of the heterogeneous 9-thiourea epiquinine catalyst is especially concerned. It has been demonstrated in our previous report [27] that SBA-15 supported 9-thiourea epiquinine exhibits enhanced enantioselectivity (up to 99%) in the asymmetric Friedel–Crafts reaction of imines with indoles, and could be recycled and regenerated readily as well.

2. Experimental

MCM-41-SH and SBA-15-SH were prepared by the post-synthesis grafting of parent mesoporous silica with 3-mercaptopropyltrimethoxysilane (MPTMS, 95%, Alfa Aesar) in anhydrous toluene. 9-(3,5-bis(trifluoromethyl)phenyl thiourea)epiquinine, synthesized according to the previous report [3], AIBN as radical initiator, and

* Corresponding author. Fax: +86 10 64425385.
E-mail address: jinghe@263.net.cn (J. He).

0021-9517/$ – see front matter
doi:10.1016/j.jcat.2008.09.006

MCM-41-SH or SBA-15-SH were refluxed in chloroform under inert atmosphere to give MCM-41-SQT or SBA-15-SQT.

The solid state NMR spectra were recorded on a Bruker Avance 300M solid-state spectrometer at resonance frequencies of 75.5 MHz for ^{13}C and 59.6 MHz for ^{29}Si. ^{1}H and ^{13}C NMR in solution were recorded on a Bruker Avance 600 spectrometer. N_2 sorption isotherms were measured on a Quantachrome Autosorb-1 system. Elemental analyses (EA) were performed on a Bruker CHNS elemental analyzer. FT-IR spectra were taken on a Bruker Vector 22 spectrometer at a resolution of 4 cm^{-1} using the standard KBr method. VCD spectrum was recorded on a Bruker Vector 22 spectrometer equipped with VCD/IRRAS model PMA37 at resolution of 4 cm^{-1}.

In a typical asymmetric Friedel–Crafts reaction, indole (99%, Aldrich, 0.2 mmol) was introduced in one portion to a suspension of *N*-benzylidenebenzenesulfonamide (99%, Aldrich, 0.1 mmol) and catalyst (1 mol% accounted by 9-thiourea epiquinine, vacuumed prior to use) in 0.3 mL of solvent, then to oscillate for 5 days. The filtrate was subjected to flash chromatography (silica gel: ethyl acetate/hexane = 1/3) to afford the desired product and unconverted imines. The same procedure was repeated except the usage of catalyst, to afford the racemic product in 17% yield. The enantiomer excess (ee) was determined on a Shimadzu LC-10Atvp HPLC with a Daicel Chiralcel OB-H column (wavelength = 254 nm) using i-PrOH/hexane (20/80, v/v) as mobile phase.

3. Results and discussion

3.1. Immobilization of 9-thiourea epiquinine on mesoporous silica

The immobilization of 9-(3,5-bis(trifluoromethyl)phenylthiourea)epiquinine on mesoporous MCM-41 or SBA-15 material is achieved using a bottom-up approach with mercapto group as a linker. The grafting of mecaptopropyl groups and the following covalent linkage of 9-(3,5-bis(trifluoromethyl)phenylthiourea) epiquinine are investigated by solid state ^{29}Si and ^{13}C NMR spectroscopy. In the ^{29}Si CP/MAS NMR spectra shown in Fig. 1 (top), SBA-15-SH presents a marked decrease in the relative intensity of Q^3 linkage at $\delta = -101$ ppm to Q^4 at $\delta = -111$ ppm, as a result of the grafting reaction between the surface silanols and silane moieties. Simultaneously, the resonances at −48, −58, and −65 ppm associated with T^1, T^2 and T^3 linkages ($T^m = (SiO)_m–Si–(OCH_3)_{3-m}R$, $m = 1–3$) are observed, further verifying the anchor of mecaptopropyl groups to silica walls. In the case of MCM-41, T^m linkages and similar change in the relative intensity of Q^3 to Q^4 are observed, except that no T^3 linkage is present for MCM-41-SH. Due to the following anchoring of 9-thiourea epiquinine, T^3 emerges and T^2 intensifies for MCM-41-SQT. For SBA-15-SQT, T^1 resonance gets weakened while both T^2 and T^3 are enhanced. As a result, the intensity of Q^3 displays a further decrease relative to Q^4 on both SBA-15-SQT and MCM-41-SQT. The secondary grafting of methoxysilane moiety (T^1 to T^2 or T^3, and T^2 to T^3) visibly occurs in the incorporation of 9-thiourea epiquinine. The relative area ratio of Q^4 to Q^3, quantitatively estimated from the solid state ^{29}Si MAS NMR spectra, is 1.6, 1.8 and 2.6 for SBA-15, SBA-15-SH and SBA-15-SQT, and 1.5, 1.9 and 5.3 for MCM-41, MCM-41-SH and MCM-41-SQT, respectively. In the ^{13}C CP/MAS NMR spectra (Fig. 1), SBA-15-SH and MCM-41-SH clearly display three resonances at 10, 27, and 48 ppm, which are absent for parent MCM-41 and SBA-15. The resonances at 10 and 27 ppm are assigned to the $–\underline{C}H_2\underline{C}H_2–CH_2SH$ and $–\underline{C}H_2–SH$ of the tethered mecaptopropyl groups. The resonance at 48 ppm originates from the residual methoxy groups due to the incomplete condensation of MPTMS [28]. For SBA-15-SQT and MCM-41-SQT, new resonances at 31, 33 ($Si–(CH_2)_3–S–\underline{C}H_2–\underline{C}H_2–$), 55 ($O–\underline{C}H_3$), 26, 39, 41, 53, 59 (quinidine), 101, 121, 125, 128, 131, 143, 158 (aromatic carbons) and 186 ppm (C=S), all characteristic of the existence of 9-(3,5-bis(trifluoromethyl)phenylthiourea)epiquinine moiety, are clearly observed, exactly as expected. The resonances at 114.0 and 141.5 ppm corresponding to C atoms in $–\underline{C}H=\underline{C}H_2$ groups are absent, indicative of the reaction between thiol groups on MCM-41-SH and SBA-15-SH surface and vinylic functional group in 9-(3,5-bis(trifluoromethyl)phenylthiourea)epiquinine. Correspondingly, in the FT-IR spectra (Supplemental material), the absorption band at 2576 cm^{-1} arising from S–H vibration emerges upon the grafting of 3-mercaptopropylsilyl group and vanishes due to the covalent linkage of 9-thiourea epiquinine moiety. The FT-IR bands at 1512, 1473, 1401, and 1383 cm^{-1} originating from the aryl rings in the anchored 9-thiourea epiquinine also appear. Obvious VCD signals that are not present for the parent SBA-15 and SBA-15-SH are observed for SBA-15-SQT (Supplemental material).

The loading of 9-thiourea epiquinine in SBA-15-SQT is typically 0.16 mmol/g calculated according to the EA results, slightly less than 0.20 mmol/g, the value estimated according to the SH content in SBA-15-SH. This means that not all SH groups in SBA-15-SH effectively took part in the linkage with 9-(3,5-bis(trifluoromethyl) phenylthiourea)epiquinine. The loading of 9-thiourea epiquinine in MCM-41-SQT is calculated as 0.20 mmol/g, which is higher than that in SBA-15-SQT. The observed difference is rationally attributed to the fact that the content of thiol group in MCM-41-SH is 0.91 mmol/g, higher than 0.74 mmol/g in SBA-15-SH. The α_s-plot analysis has been performed in this work to assess the location of organic moieties introduced onto the MCM-41 and SBA-15 surfaces. A nonporous α-quartz with a BET surface area of 1.21 m^2/g is used as reference material. The analyzed interior and exterior surface areas are presented in Table 1. Compared with parent SBA-15, the exterior surface area and the mesoporous surface area of SBA-15-SH decrease by 23 and 31%. The exterior surface area and the mesopores surface area of SBA-15-SQT decrease by 16 and 24% in comparison with that of SBA-15-SH. The decrease percentage of exterior surface area and mesoporous surface area, caused by the covalent linkage of 9-thiourea epiquinine to SBA-15-SH, is both 7%. It could thus be deduced that 9-thiourea epiquinine has been incorporated comparably on the interior and exterior surfaces of SBA-15-SH. In the case of MCM-41, the grafting of mecaptopropyl groups decreases the exterior surface area and mesopores surface area in 9.3 and 17.6%. The following incorporation of 9-thiourea epiquinine reduces the exterior surface area and the mesopores surface area in 9.3 and 2.4%. The interior surface area is reduced in less percentage than exterior surface area in the incorporation of 9-thiourea epiquinine, which is closely associated with the smaller pore size of MCM-41 materials. The heterogenization of 9-thiourea epiquinine might give rise to partial blocking of MCM-41 channels. Or more severe diffusion resistance in the smaller pores makes 9-thiourea epiquinine anchored on the exterior surface more readily. The quantity of Si–OH on the exterior surface of MCM-41 is calculated as 0.62 mmol/g based on the ^{29}Si MAS NMR spectrum. The maximum quantity of –SH groups on the exterior surface is thus 0.31 mmol/g, supposed that the external Si–OH is entirely grafted. The estimated content of 9-thiourea epiquinine on the exterior surface is larger than actually observed in MCM-41-SQT (0.20 mmol/g).

The grafting of mecaptopropyl groups and the following incorporation of 9-thiourea epiquinine make no adverse impacts on the long-range ordered structure. All of the materials exhibit well-defined type IV isotherms with sharp steeps and H1-type hysteresis loops (Supplemental material), which is characteristic of well-ordered mesoporous channels. The surface area, pore volume, and pore size at maximum distribution is gradually reduced with stepwise introduction of organic groups, as shown in Table 1. The increasing wall thickness coincides with the stepwise linkage of organic moieties on the surfaces. The mercapto-functionalized in-

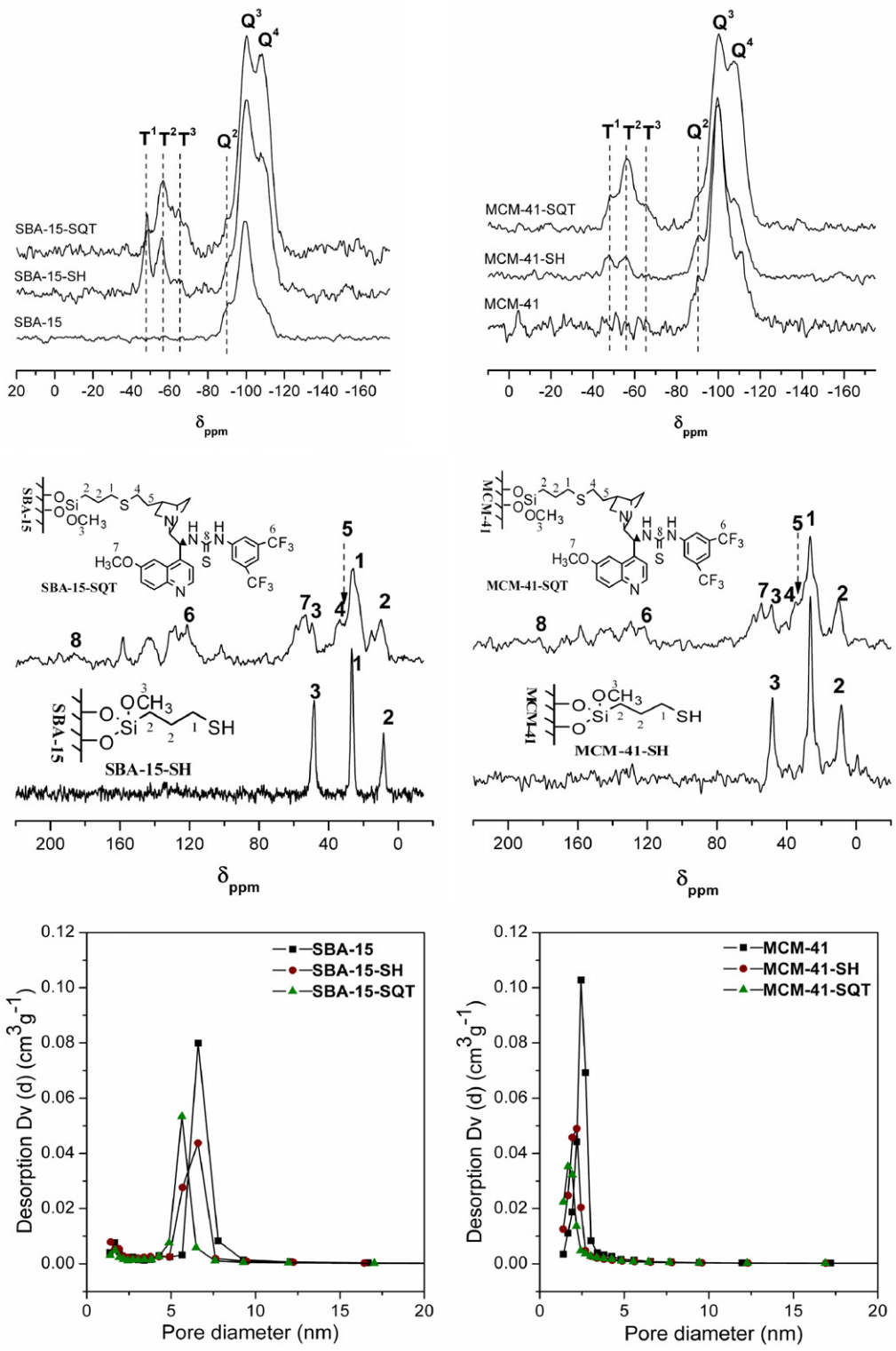

Fig. 1. ^{29}Si (top) and ^{13}C (middle) CP/MAS NMR spectra, pore size distribution (bottom) calculated using Barrett–Joyner–Halenda (BJH) method based on the desorption branch.

termediates and the resulting heterogeneous catalysts all possess the pore size distributions as narrow as the parent mesoporous materials, as can be seen in Fig. 1 (bottom).

3.2. Catalytic property of heterogeneous 9-thiourea epiquinine catalysts

The catalytic activities and enantioselectivities of MCM-41-SQT and SBA-15-SQT are evaluated by the asymmetric Friedel–Crafts reaction of indoles with imines. The reaction of indole (**1a**) with *N*-benzylidenebenzenesulfonamide (**2a**) in various solvents was first performed using SBA-15-SQT as catalyst (Table 2). The reactions at ambient temperature in EtOAc (entry 6) and toluene (entry 2) afford the corresponding *N*-(indol-3-yl-phenylmethyl)benzenesulfonamide (**3aa**) in nearly 100 and 96% *ee*. The reaction in THF (entry 5) turns out racemic product. The other solvents lead to moderate enantioselectivity and the products with

Table 1
The mesoporous surface areas and exterior surface areas analyzed by α_s-plot method, and the textural properties determined from N_2 adsorption experiments.

Sample	S_{ex} (m^2/g)[a]	S_{meso} (m^2/g)[b]	S_{BET} (m^2/g)[c]	Pore volume (cm^2/g)[d]	Pore diameter (nm)[e]	Wall thickness (nm)
SBA-15	59	736	778	1.3	6.6	4.7
SBA-15-SH	45	504	544	0.9	6.5	6.1
SBA-15-SQT	38	383	395	0.7	5.7	6.7
MCM-41	107	902	1014	1.9	2.5	2.2
MCM-41-SH	97	743	822	0.9	2.2	2.2
MCM-41-SQT	88	725	622	0.8	1.7	2.8

[a] Exterior surface area by α_s-plot analysis.
[b] Mesoporous surface area by α_s-plot analysis.
[c] Specific surface area calculated using Brunauer–Emmett–Teller method based on the adsorption branch of N_2 sorption isotherms.
[d] Single point pore volume estimated from the adsorbed amount at $p/p_0 = 0.99$.
[e] The maximum in pore size distribution calculated using Barrett–Joyner–Halenda (BJH) method based on the desorption branch of N_2 sorption isotherms.

reversed configuration. MeOH, toluene, MeCN, and EtOAc as solvents give a chemical selectivity above 60% in each case. But the reaction in MeOH (entry 1), toluene (entry 2), or MeCN (entry 3) produces the desired product (**3aa**) in a yield of below 50% because of the unsatisfactory reactivity (low conversion). THF or CH_2Cl_2 as solvent turns out deficient activity and as well chemical selectivity. Although EtOAc was generally considered a poor solvent in hydrogen-bonding controlled organocatalysis, good yield and enantioselectivity are produced using EtOAc as solvent in our case. Wittkopp and Schreiner [29] have previously reported similar observations in homogeneous thiourea-catalyzed Diels–Alder reactions. They found that the strong catalytic effectiveness was also present in highly coordinating polar solvents, such as water. Moderate increase in the reaction temperature in EtOAc retains the enantioselectivity while enhances the yield (entry 7). Further elevating the reaction temperature to 50 °C (entry 8), however, causes a marked decrease in the yield, arising from the decrease in the chemical selectivity. The following experiments are thus performed at 40 °C using EtOAc as solvent.

Both indoles and imines have been screened as the substrates for the asymmetric Friedel–Crafts reaction. As shown in Table 2, 6-OCH_3 (entry 9) and 5-CH_3 (entry 10) substituted indoles proceed with the addition reaction successfully. The observed chemical selectivity and *ee* slightly decrease with increased dimension of indole molecules. It could rationally be explained by the fact that smaller molecules diffuse into the support channels more easily. The reaction taking place inside the channels turns out better chemical selectivity and enantioselectivity. Altering the *N*-protecting group in imine from –Bs (entry 7) to –Ts (entry 11) reduces the yield, chemical selectivity, and *ee*. When the aryl group (entry 11) is replaced by an alkyl group (entry 12), enhanced chemical selectivity, yield and *ee* are observed. The effects of imine structures on the Friedel–Crafts reaction could also be well interpreted by the reasons proposed in the discussion of indole effects. The reaction inside the nano-sized channels involving smaller imine molecules, –Bs (relative to –Ts) or alkyl (relative to aryl) substituted for example, favors both chemical selectivity and enantioselectivity. It has been found in our previous research [27] that electron-attracting –Cl or $-NO_2$ substituted benzylidene moiety inhibits the occurrence of addition reaction. No products could be detected in the reaction mixture.

Both MCM-41-SQT and SBA-15-SQT catalysts efficiently promote the enantioselective reaction of indole with *N*-benzylidenebenzenesulfonamide, as shown in Table 3 (entries 2 and 3), producing higher chiral induction (96 and 99% *ee*) than their homogeneous counterpart (entry 1, 93% *ee*). The simple mixture of SBA-15-SH and 9-(3,5-bis(trifluoromethyl)phenylthiourea)epiquinine as catalyst turns out similar reactive effectiveness and chiral induction (entry 4) to the homogeneous system (entry 1), indicative of the close relationship between the enhancement of enantioselectivity and the covalent attachment of 9-thiourea epiquinine to the support surfaces. Similar behavior has been reported earlier on supported chiral Mn(III) and Cr(III) complexes [21,22,30]. The MCM-41-SQT catalyst is more active while less chemically selective and asymmetrically inductive than SBA-15-SQT, proposed to arise from the difference in the location of catalytic sites. The catalytic sites located mainly on the exterior surface of MCM-41 are

Table 2
Asymmetric Friedel–Crafts reactions of indoles with imines on SBA-15 supported 9-thiourea epiquinine:

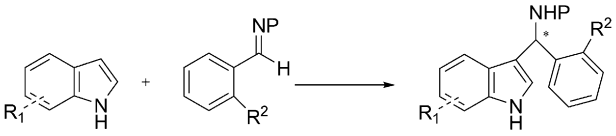

P=Ts or Bs (Bs=SO_2Ph)

1 2 3

Entry	Solvent	T (°C)	1	2	3	Conv. (%)[a]	Sel. (%)[b]	Yield (%)[c]	*ee* (%)[c]
1	MeOH	30	1a: $R^1 = H$	2a: $R^2 = H$, P = Bs	3aa	54	81	44	56
2	Toluene	30	1a: $R^1 = H$	2a: $R^2 = H$, P = Bs	3aa	30	79	24	96
3	MeCN	30	1a: $R^1 = H$	2a: $R^2 = H$, P = Bs	3aa	46	65	30	84
4	CH_2Cl_2	30	1a: $R^1 = H$	2a: $R^2 = H$, P = Bs	3aa	28	25	7	87
5	THF	30	1a: $R^1 = H$	2a: $R^2 = H$, P = Bs	3aa	42	24	10	Null
6	EtOAc	30	1a: $R^1 = H$	2a: $R^2 = H$, P = Bs	3aa	77	92	71	99
7	EtOAc	40	1a: $R^1 = H$	2a: $R^2 = H$, P = Bs	3aa	83	93	77	99
8	EtOAc	50	1a: $R^1 = H$	2a: $R^2 = H$, P = Bs	3aa	71	42	30	98
9	EtOAc	40	1b: R^1 = 6-OMe	2a: P = Bs, $R^2 = H$	3ba	76	91	69	99
10	EtOAc	40	1c: R^1 = 5-Me	2a: P = Bs, $R^2 = H$	3ca	77	86	66	93
11	EtOAc	40	1a: $R^1 = H$	2b: P = Ts, $R^2 = H$	3ab	80	85	68	90
12	EtOAc	40	1a: $R^1 = H$	2c: 	3ae	86	93	80	96

[a] Conversion calculated as the molar percentage of the reacted in the total imines.
[b] Chemselectivity determined as the molar percentage of the imines converted into the desired product in all the reacted imines.
[c] Isolated desired products.

Table 3
Asymmetric Friedel–Crafts reactions of indole with imine:

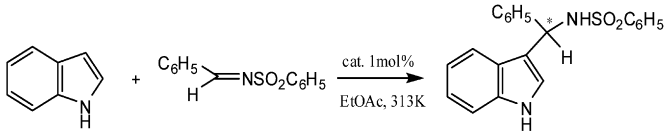

Entry	Catalyst	Conv. (%)[b]	Sel. (%)[c]	Yield (%)[d]	*ee* (%)[d]
1	Homogeneous counterpart[a]	92	84	77	93
2	SBA-15-SQT	83	93	77	99
3	MCM-41-SQT	87	90	78	96
4	Physical mixture of SBA-15-SH and homogeneous counterpart	92	80	74	92

[a] 9-(3,5-bis(trifluoromethyl)phenylthiourea)epiquinine.
[b] Conversion calculated as the molar percentage of the reacted in the total imines.
[c] Chemselectivity determined as the molar percentage of the imines converted into the desired product in all the reacted imines.
[d] Isolated desired products.

more accessible. But the catalytic sites in the mesopores, in the case of SBA-15-SQT, favor the chemical selectivity and enantioselectivity.

4. Conclusions

In summary, the 9-thiourea epiquinine supported on MCM-41 and SBA-15 exhibits the reactivity, chemical selectivity and chiral induction as excellent as the homogeneous counterpart in the asymmetric Friedel–Crafts reaction of indoles with imines. With the chiral sites anchored comparably in the nano-sized channels and exterior surface, SBA-15-SQT exhibits higher chemical selectivity and asymmetrical induction but lower conversion slightly than MCM-41-SQT, in which the catalytic sites are located preferentially on the exterior surface. The substrate screening finds that the molecule dimensions of both indoles and imines make impact on the chemical selectivity and enantioselectivity.

Acknowledgments

The authors are grateful to the financial support from NSFC, Program for Changjiang Scholars and Innovative Research Team in University (IRT0406), and “111” Project (B07004).

Supplementary material

Supplementary material of this article may be found on ScienceDirect in the online version.

Please visit doi: 10.1016/j.jcat.2008.09.006.

References

[1] S.J. Connon, Chem. Eur. J. 12 (2006) 5418.
[2] J. López-Cantarero, M.B. Cid, T.B. Poulsen, M. Bella, J.L.G. Ruano, K.A. Jørgensen, J. Org. Chem. 72 (2007) 7062.
[3] B. Vakulya, S. Varga, A. Csámpai, T. Soós, Org. Lett. 7 (2005) 1967.
[4] J. Wang, H. Li, L. Zu, W. Jiang, H. Xie, W. Duan, W. Wang, J. Am. Chem. Soc. 128 (2006) 12652.
[5] G. Bartoli, M. Bosco, A. Carlone, A. Cavalli, M. Locatelli, A. Mazzanti, P. Ricci, L. Sambri, P. Melchiorre, Angew. Chem. Int. Ed. 45 (2006) 4966.
[6] B. Wang, F. Wu, F. Wang, X. Liu, L. Deng, J. Am. Chem. Soc. 129 (2007) 768.
[7] M.M. Biddle, M. Lin, K.A. Scheidt, J. Am. Chem. Soc. 129 (2007) 3830.
[8] P. Elsner, L. Bernardi, G.D. Salla, J. Overgaard, K.A. Jørgensen, J. Am. Chem. Soc. 130 (2008) 4897.
[9] J.-X. Ye, D.J. Dixon, P.S. Hynes, Chem. Commun. (2005) 4481.
[10] S.H. McCooey, S.J. Connon, Angew. Chem. Int. Ed. 44 (2005) 6367.
[11] A.L. Tillman, J. Ye, D.J. Dixon, Chem. Commun. (2006) 1191.
[12] T. Liu, H. Cui, J. Long, B.-J. Li, Y. Wu, L. Ding, Y.-C. Chen, J. Am. Chem. Soc. 129 (2007) 1878.
[13] B. Török, M. Abid, G. London, J. Esquibel, M. Török, S.C. Mhadgut, P. Yan, G.K.S. Prakash, Angew. Chem. Int. Ed. 44 (2005) 3086.
[14] Y.Q. Wang, J. Song, R. Hong, H. Li, L. Deng, J. Am. Chem. Soc. 128 (2006) 8156.
[15] L. Bernardi, F. Fini, R.P. Herrera, A. Riccia, V. Sgarzani, Tetrahedron 62 (2006) 375.
[16] D. Pettersen, F. Piana, L. Bernardi, F. Fini, M. Fochi, V. Sgarzani, A. Ricci, Tetrahedron Lett. 48 (2007) 7805.
[17] Y. Wang, H.-M. Li, Y.-Q. Wang, Y. Liu, B.M. Foxman, L. Deng, J. Am. Chem. Soc. 129 (2007) 6364.
[18] F. Cozzi, Adv. Synth. Catal. 348 (2006) 1367.
[19] C.E. Song, S. Lee, Chem. Rev. 102 (2002) 3495.
[20] M. Benaglia, A. Puglisi, F. Cozzi, Chem. Rev. 103 (2003) 3401.
[21] S. Xiang, Y. Zhang, Q. Xin, C. Li, Chem. Commun. (2002) 2696.
[22] X.-G. Zhou, X.-Q. Yu, J.-S. Haung, S.-G. Li, L.-S. Li, C.-M. Che, Chem. Commun. (1999) 1789.
[23] B.F.G. Johnson, S.A. Raynor, D.S. Shephard, T. Mashmeyer, J.M. Thomas, G. Sankar, S. Bromley, R. Oldroyd, L. Gladdenc, M.D. Mantlec, Chem. Commun. (1999) 1167.
[24] M.D. Jones, R. Raja, J.M. Thomas, B.F.G. Johnson, D.W. Lewis, J. Rouzaud, K.D.M. Harris, Angew. Chem. Int. Ed. 42 (2003) 4326.
[25] H.D. Zhang, Y.M. Zhang, C. Li, J. Catal. 238 (2006) 369.
[26] R.I. Kureshy, I. Ahmad, N.H. Khan, S.H.R. Abdi, K. Pathak, R.V. Jasra, J. Catal. 238 (2006) 134.
[27] P. Yu, J. He, C.-X. Guo, Chem. Commun. (2008) 2355.
[28] V. Dufaud, M.E. Davis, J. Am. Chem. Soc. 125 (2003) 9403.
[29] A. Wittkopp, P.R. Schreiner, Chem. Eur. J. 9 (2003) 407.
[30] R.I. Kureshy, I. Ahmad, N.H. Khan, S.H.R. Abdi, S. Singh, P.H. Pandia, R.V. Jasra, J. Catal. 235 (2005) 28.